

See discussions, stats, and author profiles for this publication at: <https://www.researchgate.net/publication/51635331>

Berichtigung: NaSr₃Be₃B₃O₉F₄: A Promising Deep-Ultraviolet Nonlinear Optical Material Resulting from the Cooperative Alignment of the [Be₃B₃O₁₂F]₁₀ – Anionic Group

ARTICLE in ANGEWANDTE CHEMIE INTERNATIONAL EDITION · SEPTEMBER 2011

Impact Factor: 11.26 · DOI: 10.1002/anie.201103960 · Source: PubMed

CITATIONS

80

READS

87

8 AUTHORS, INCLUDING:



Hongwei Huang

China University of Geosciences (Beijing)

83 PUBLICATIONS 636 CITATIONS

SEE PROFILE



Jiyong Yao

Chinese Academy of Sciences

122 PUBLICATIONS 900 CITATIONS

SEE PROFILE



Zheshuai Lin

Chinese Academy of Sciences

170 PUBLICATIONS 2,588 CITATIONS

SEE PROFILE



Geng Chao

Chinese Academy of Sciences

40 PUBLICATIONS 260 CITATIONS

SEE PROFILE

NaSr₃Be₃B₃O₉F₄: A Promising Deep-Ultraviolet Nonlinear Optical Material Resulting from the Cooperative Alignment of the [Be₃B₃O₁₂F]^{10−} Anionic Group**

Hongwei Huang, Jiyong Yao, Zheshuai Lin, Xiaoyang Wang, Ran He, Wenjiao Yao, Naixia Zhai, and Chuangtian Chen*

The demand for deep-ultraviolet (deep-UV) coherent light sources ($\lambda < 200$ nm) has become increasingly urgent because they have important applications in semiconductor photolithography, laser micromachining, modern scientific instruments (super-high-resolution and angle-resolved photoemission spectrometer, for example) and so forth. To date, the most effective method to generate deep-UV coherent light with solid-state lasers is through cascaded frequency conversion, in particular multiharmonics, using deep-UV nonlinear optical (NLO) crystals. Therefore, the discovery of suitable deep-UV NLO crystals is of great importance.

In the past decades, the anionic group theory,^[1–3] which reveals that the overall nonlinearity of a crystal is the geometrical superposition of the microscopic second-order susceptibility tensors of the NLO-active anionic groups, has been very successful in developing borate NLO crystals. Several important NLO crystals have been discovered, including β -BaB₂O₄ (BBO),^[4] LiB₃O₅ (LBO),^[5] CsB₃O₅ (CBO),^[6] CsLiB₆O₁₀ (CLBO),^[7,8] and YCa₄O(BO₃)₃ (YCOB),^[9] which have been widely used in NLO optics. However, they cannot be used to generate deep-UV coherent light ($\lambda < 200$ nm) by multiharmonic generation owing to some inherent shortcomings. Thus, the search for new NLO materials, particularly for deep-UV applications, has attracted considerable attention.^[10–14]

A deep-UV NLO material must have a very short absorption edge, and in this respect, beryllium borates are attractive as they are supposed to possess very large energy gap.^[15] It is also well known that the incorporation of fluorine can effectively cause the UV absorption edge of a crystal to blue-shift, so our group has made great efforts to search for new deep-UV NLO fluorine beryllium borate crystals. After more than ten years of intensive research in our group, the KBe₂BO₃F₂^[16–18] (KBBF) crystal became the first practically usable deep-UV NLO crystal used to generate coherent 177.3

and 193 nm light. The excellent NLO properties of KBBF crystals are mainly determined by the (Be₂BO₃F₂)_∞ layer made up of trigonal-planar [BO₃] units and the tetrahedral [BeO₃F] units. This deep-UV coherent light material has been used as a photon source in modern instruments and revealed many novel scientific phenomena which could not be observed by traditional techniques, as shown in the study of superconductor CeRu₂^[19] and Bi₂Sr₂CaCu₂O_{8+δ}.^[20] Unfortunately, the KBBF crystal is very difficult to grow in thickness because of its strong layering tendency, which severely limits the coherent output power. Therefore, there is great demand for new types of fluorine beryllium borates which have deep-UV transmission, moderate birefringence, and relatively large second harmonic generation (SHG) coefficients, and at the same time overcome the crystal-growth problems found in the KBBF crystal.

Alkali-metal and alkaline-earth-metal cations are favorable for the transmission of UV light because there are no d–d electron or f–f electron transitions in this spectral region. As shown in numerous explorations, the size and charge of cations have great influence on the macroscopic packing of anions, which in turn determines the overall NLO properties in a crystal.^[21,22] Herein, we utilize both alkali-metal and alkaline-earth-metal cations. Different charge/size combinations of mixed cations may have different influences on the packing of anions, so it is more likely to isolate new phases with interesting stoichiometries, structures, and properties. To date, no fluorine beryllium borates with mixed cations have been reported. Guided by this idea, we successfully obtained a new alkali-metal/alkaline-earth-metal fluorine beryllium borate NaSr₃Be₃B₃O₉F₄, which contains the novel anionic group [Be₃B₃O₁₂F]^{10−} as the basic building unit. Furthermore, the arrangement of these [Be₃B₃O₁₂F]^{10−} groups is very favorable for generating large a NLO response and moderate birefringence and especially for avoiding the layering tendency during bulk crystal growth. Herein, we report the synthesis, crystal growth, structure, linear and nonlinear optical properties, thermal behavior, and electronic structure of NaSr₃Be₃B₃O₉F. These results indicate that the NaSr₃Be₃B₃O₉F₄ crystal may be a promising NLO material in the deep-UV range.

NaSr₃Be₃B₃O₉F₄^[23] crystallizes in the noncentrosymmetric trigonal space group R3m. The crystal structure is depicted in Figure 1a. In the asymmetric unit, Sr, Na, Be, B each occupy one crystallographically unique position, and there are two unique F and O positions. The B atom is coordinated to three O atoms to form a planar BO₃ unit with B–O bond lengths

[*] H. Huang, J. Yao, Z. Lin, X. Wang, R. He, W. Yao, N. Zhai, Prof. C. Chen
Center for Crystal Research and Development
Technical Institute of Physics and Chemistry
Chinese Academy of Sciences, Beijing 100190 (China)
E-mail: cct@mail.ipc.ac.cn

[**] This work was supported by the National Natural Science Foundation of China under Grant Nos. 50590402 and 91022036 and by the National Basic Research Project of China (No. 2010CB630701, and 2011CB922204).

Supporting information for this article is available on the WWW under <http://dx.doi.org/10.1002/anie.201103960>.

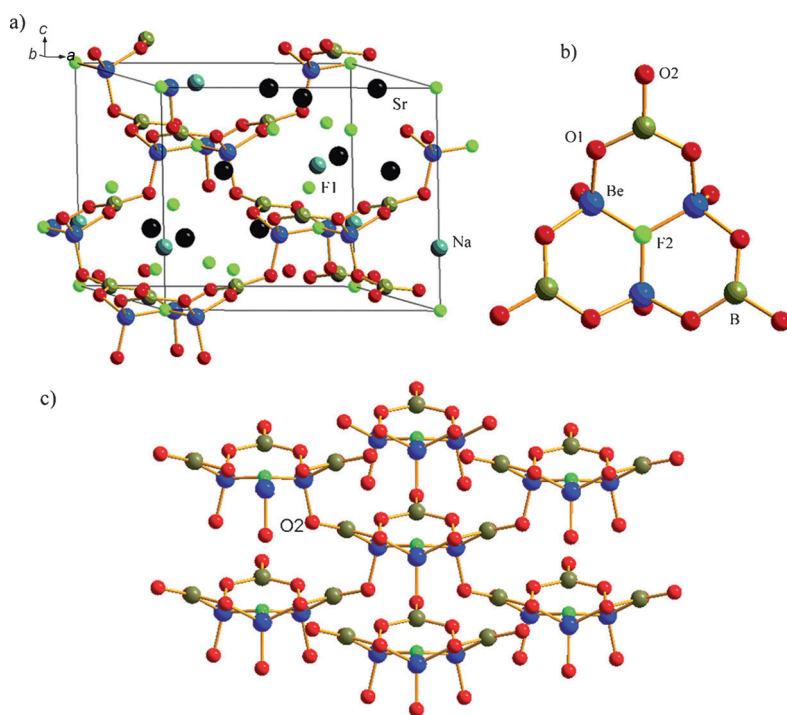


Figure 1. a) Crystal structure of $\text{NaSr}_3\text{Be}_3\text{B}_3\text{O}_9\text{F}_4$. b) Anionic group $[\text{Be}_3\text{B}_3\text{O}_{12}\text{F}]^{10-}$. c) The connections of the $[\text{Be}_3\text{B}_3\text{O}_{12}\text{F}]^{10-}$ rings in the structure.

varying from 1.364(4) to 1.398(8) Å and O–B–O bond angles from 117.6(3) to 124.8(6)°. The Be atom is bound to three O atoms and one F atom to form a BeO_3F tetrahedron with a Be–F bond length of 1.545(7) Å and the Be–O separations ranging from 1.561(9) to 1.582(5) Å. The basic structural unit is a very unusual $[\text{Be}_3\text{B}_3\text{O}_{12}\text{F}]^{10-}$ ring (Figure 1b). Three BO_3 groups and three BeO_3F tetrahedra are alternately connected through the shared atom O1 atom to generate three six-membered rings, which are joined together by the F2 atoms. The absence of strong absorption between 3000 and 3600 cm^{-1} in the IR spectrum (see Supporting Information) along with the fact that the crystal was obtained under high-temperature solid-state conditions ruled out the possibility of hydroxy groups at the F positions. Besides, the calculated bond valence of the Be–F2 bond is 0.49, thus indicating a relatively strong covalent bond.^[24,25] The $[\text{Be}_3\text{B}_3\text{O}_{12}\text{F}]^{10-}$ ring belongs to the C_{3v} point group with a three-fold axis passing through the F2 atoms and three mirror planes passing through the Be, B, and F2 atoms. This type of structural unit is observed for the first time in fluorine beryllium borates.

Each $[\text{Be}_3\text{B}_3\text{O}_{12}\text{F}]^{10-}$ ring is further connected to six other such rings through the O2 atoms (Figure 1c). Although these $[\text{Be}_3\text{B}_3\text{O}_{12}\text{F}]^{10-}$ rings are not arranged exactly parallel to each other, they are roughly parallel to each other. The $[\text{Be}_3\text{B}_3\text{O}_{12}\text{F}]^{10-}$ rings are connected to form a three-dimensional framework with Sr^{2+} , Na^+ , and the other isolated F1^- ions present in the cavities, which is very favorable for generating a large NLO response and sufficient birefringence, and especially for the crystal growth. In the structure of the practical deep-UV NLO KBBF crystal, the active NLO layers $(\text{Be}_2\text{BO}_3\text{F}_2)_\infty$ joined together through weak electrostatic attraction of K and F atoms leads to a strong layering

tendency, which is unfavorable for growing thick crystals. In contrast, the $[\text{Be}_3\text{B}_3\text{O}_{12}\text{F}]^{10-}$ rings are connected to each other along the *c* axis through the covalently bonded Be–O–B bridge. This spatial arrangement is expected to be responsible for the weaker layering tendency and is conducive to bulk crystal growth. Our preliminary crystal growth attempts have resulted in crystals in the size of $20 \times 20 \times 10 \text{ mm}^3$ (see the Supporting Information). Therefore, $\text{NaSr}_3\text{Be}_3\text{B}_3\text{O}_9\text{F}_4$ is worthy of in-depth investigation as a promising deep-UV NLO crystal. It should be pointed out that $\text{Na}^+/\text{Sr}^{2+}$ ions are the “right” combination of mixed cations to sustain the stability of the anionic framework, as no isostructural compounds with other alkali-metal or alkaline-earth-metal cations were identified during our exploration.

The curves of the powder SHG signals as a function of particle size were detected and compared with that of KH_2PO_4 (KDP, Figure 2a). The results were consistent with the phase-matching behavior according to the rule proposed by Kurtz and Perry.^[26] The second-harmonic signal of $\text{NaSr}_3\text{Be}_3\text{B}_3\text{O}_9\text{F}_4$ was found to be about four times as large as that of KDP standard. The large NLO effect is approximately

three times as large as that of KBBF.^[27]

The UV optical transmittance spectrum of $\text{NaSr}_3\text{Be}_3\text{B}_3\text{O}_9\text{F}_4$ was recorded at room temperature on a crystal of size $5 \times 2.5 \times 1 \text{ mm}^3$ that was polished on both sides. As shown in Figure 2b, the UV short-wavelength absorption edge of $\text{NaSr}_3\text{Be}_3\text{B}_3\text{O}_9\text{F}_4$ is located at 170 nm, which is slightly red-shifted compared with the universally used crystals LBO (155 nm) and KBBF (150 nm), but much shorter than that of BBO (189 nm). The short absorption edge indicates promising prospects for application in the deep-UV range. Obviously, our transmittance measurement on a single crystal gives more accurate results than the powder diffuse reflectance method.^[10]

Differential scanning calorimetric (DSC) measurements were carried out with ground crystals of $\text{NaSr}_3\text{Be}_3\text{B}_3\text{O}_9\text{F}_4$ (see the Supporting Information). The DSC curve exhibits one endothermic peak on the heating curve at 851 °C. The XRD pattern of melted residues mainly displayed a BeO peak and was clearly different from that of the original crystals. The result demonstrates that $\text{NaSr}_3\text{Be}_3\text{B}_3\text{O}_9\text{F}_4$ is an incongruently melting compound. Therefore, it must be grown under the melting temperature by flux methods.

The partial density of state (PDOS) for $\text{NaSr}_3\text{Be}_3\text{B}_3\text{O}_9\text{F}_4$ is shown in Figure 3a, in which only the upper region of the valence band (VB) and the bottom of conduction band (CB) are shown, since the optical properties of a crystal in the visible and UV spectrum are mainly determined by the states close to the band gap.^[28] It is clear that in these states the contribution from the orbitals of the alkali-metal and alkaline-earth-metal cations is negligibly small, despite the fact that the orbitals of the larger cation becomes slightly significant at the bottom of the CB. Meanwhile, the Be

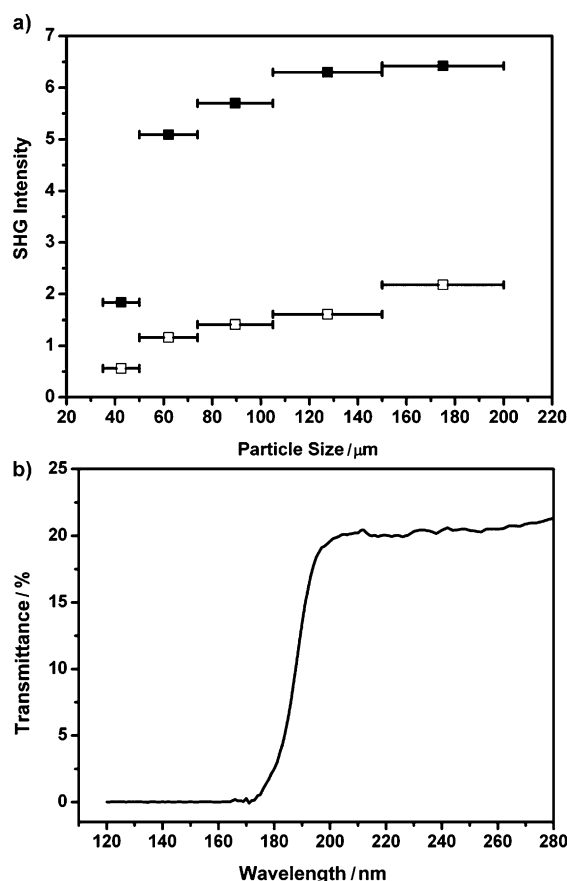


Figure 2. a) SHG measurements of NaSr₃Be₃B₃O₉F₄ ground crystals (■) with KDP (□) as reference. b) Transmittance of a NaSr₃Be₃B₃O₉F₄ crystal in the UV region.

orbitals also have very small contributions to the states close to the band gap, and the F orbitals are distributed below 2.5 eV from the VB maximum. The VB maximum and CB minimum are composed of the O 2p and B 2p orbitals, respectively, thus indicating that the optical transition between these states (in the BO₃ groups) indeed determines the main optical properties of the crystal.

Based on the electronic structure, the dispersions of the linear refractive indices for this crystal are calculated, as displayed in Figure 3b. NaSr₃Be₃B₃O₉F₄ is a negative uniaxial crystal with birefringence $\Delta n = 0.0567$ at 800 nm. Furthermore, our ab initio calculations reveal that the SHG coefficients for NaSr₃Be₃B₃O₉F₄ are $d_{11} = -d_{12} = 1.32 \text{ pm V}^{-1}$, and $d_{33} = -0.52 \text{ pm V}^{-1}$, approximately three times as large as that of KDP. The calculated values are consistent with the experimental measurements.

These optical properties can be elucidated from the microscopic structural features of NaSr₃Be₃B₃O₉F₄ crystal, shown as follows: According to the anionic group theory, in the alkali-metal and alkaline-earth-metal borate crystals, the B–O groups are the dominating active microscopic units, which determine the birefringence and SHG coefficient.^[29] In NaSr₃Be₃B₃O₉F₄, all of the [BO₃] groups are in nearly the same plane normal to the *c* axis with dihedral angles less than 20° (see Figure 1a). So its anisotropic response to the incident light is moderate ($\Delta n \approx 0.06$). By comparison, the

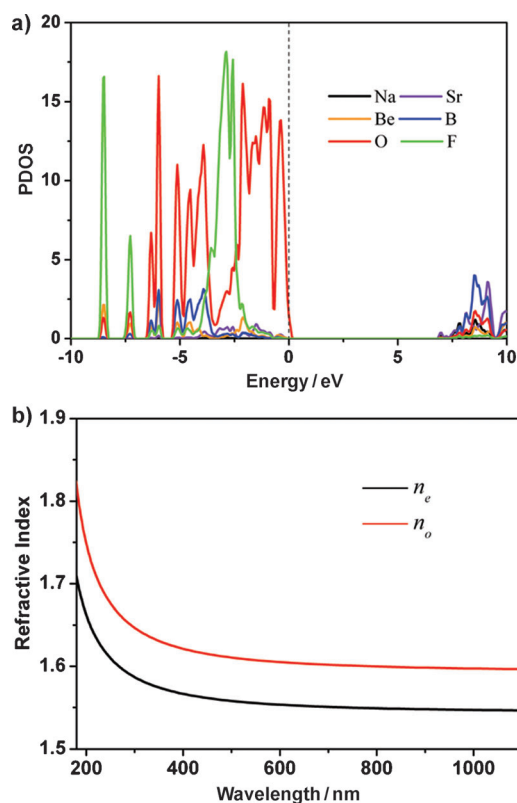


Figure 3. a) Partial density of states (PDOS) for NaSr₃Be₃B₃O₉F₄. b) Refractive indices curves for NaSr₃Be₃B₃O₉F₄. e = extraordinary, o = ordinary.

perfect in-plane (BO₃) arrangement could result in larger birefringence about 0.08 as in the case of KBBF.^[17] On the other hand, in NaSr₃Be₃B₃O₉F₄ the [BO₃] groups are almost aligned in the *ab* plane (see Figure 1b). Therefore, the microscopic second-order susceptibilities of [BO₃] groups are positively superimposed in NaSr₃Be₃B₃O₉F₄, which makes the SHG coefficients of NaSr₃Be₃B₃O₉F₄ quite large.

In conclusion, the first mixed-cation fluorine beryllium borate NaSr₃Be₃B₃O₉F₄ has been found and crystals were successfully grown with B₂O₃ and NaF as flux media. The crystal structure of NaSr₃Be₃B₃O₉F₄ features a novel anionic group [Be₃B₃O₁₂F]¹⁰⁻ consisting of three hexatomic rings joined together by F2 atoms. The [Be₃B₃O₁₂F]¹⁰⁻ rings are further connected to form a three-dimensional framework with Sr²⁺, Na⁺, and F¹⁻ ions present in the cavities, which is favorable for generating a large NLO response and moderate birefringence, and especially for the bulk crystal growth. Our preliminary crystal-growth attempts have resulted in crystals of size 20 × 20 × 10 mm³. Powder SHG test on ground crystals reveals that NaSr₃Be₃B₃O₉F₄ is phase-matchable with strong SHG signal intensity approximately four to five times as large as that of KDP. The UV transmittance measurement on a single crystal demonstrates that NaSr₃Be₃B₃O₉F₄ possesses a short-wavelength absorption edge of 170 nm. According to theoretical calculations, the BO₃ groups determine the main optical properties of the crystal. Our preliminary investigation indicates that NaSr₃Be₃B₃O₉F₄ is a promising deep-UV NLO crystalline material.

Experimental Section

$\text{NaSr}_3\text{Be}_3\text{B}_3\text{O}_9\text{F}_4$ was obtained by spontaneous crystallization using B_2O_3 and NaF as flux media from 760 to 700 °C by cooling the melt at a rate of 1 °C per day (see the Supporting Information). Elemental analysis: Na/Sr/Be/B = 1:2.6:2.8:3.1.

The thermal properties of $\text{NaSr}_3\text{Be}_3\text{B}_3\text{O}_9\text{F}_4$ were investigated by differential scanning calorimetric (DSC) analysis using a Labsys TG-DTA16 (SETARAM) thermal analyzer calibrated with Al_2O_3 . A sample (10 mg) of ground crystals was placed in a platinum crucible and heated from room temperature to 1250 °C at a rate of 10 °C min⁻¹ in nitrogen atmosphere. The melted residues were examined and analyzed by X-ray powder diffraction after the experiments.

Second-harmonic generation (SHG) test was performed on ground crystals of $\text{NaSr}_3\text{Be}_3\text{B}_3\text{O}_9\text{F}_4$ by means of the Kurtz–Perry method.^[26] The sample was irradiated with a pulsed infrared beam (10 ns, 3 mJ, 10 kHz) produced by a Q-switched Nd:YAG laser at a wavelength of 1064 nm. As the powder SHG effect depends strongly on the particle size, $\text{NaSr}_3\text{Be}_3\text{B}_3\text{O}_9\text{F}_4$ crystals were ground and sieved into the following particle size ranges: 35–50, 50–74, 74–105, 105–150, and 150–200 µm. Microcrystalline KH_2PO_4 (KDP) samples within the corresponding size ranges served as the standard.

The UV optical transmittance spectrum was measured at room temperature using a spectrophotometer (VUVas2000, McPherson) in the wavelength range 120–380 nm.

The electronic structures as well as the linear and nonlinear optical properties of the $\text{NaSr}_3\text{Be}_3\text{B}_3\text{O}_9\text{F}_4$ crystal were obtained by the plane-wave pseudopotential method,^[30,31] which has been successfully applied on many borate NLO crystals.^[29] The optimized norm-conserving pseudopotentials^[32] in the Kleinman–Bylander form^[33] for Na, Sr, Be, B, O, and F are used to ensure a small plane-wave basis set without compromising the accuracy. Local density approximation (LDA) with a very high kinetic energy cutoff of 900 eV is adopted. Monkhorst–Pack *k*-point meshes^[34] with a density of (2 × 2 × 2) points in the Brillouin zone of the $\text{NaSr}_3\text{Be}_3\text{B}_3\text{O}_9\text{F}_4$ unit cell were chosen. Tests show that the total energy with the above computational parameters is accurate to 15 meV atom⁻¹, which is adequate for the current studies.

Received: June 10, 2011

Published online: August 24, 2011

Keywords: borates · electronic structure · nonlinear optics · solid-state structures · structure–property relationships

- [1] C. T. Chen, *Sci. Sin.* **1979**, 22, 756.
- [2] C. T. Chen, G. Z. Liu, *Annu. Rev. Mater. Sci.* **1986**, 16, 203.
- [3] C. T. Chen, Y. C. Wu, R. K. Li, *Int. Rev. Phys. Chem.* **1989**, 8, 65.
- [4] C. T. Chen, B. C. Wu, A. D. Jiang, G. M. You, *Sci. Sin. Ser. B* **1985**, 28, 235.
- [5] C. T. Chen, Y. C. Wu, A. D. Jiang, B. C. Wu, G. M. You, R. K. Li, S. J. Lin, *J. Opt. Soc. Am. B* **1989**, 6, 616.
- [6] Y. C. Wu, T. Sasaki, S. Nakai, A. Yokotani, H. G. Tang, C. T. Chen, *Appl. Phys. Lett.* **1993**, 62, 2614.
- [7] Y. Mori, I. Kuroda, S. Nakajima, T. Sasaki, S. Nakai, *Appl. Phys. Lett.* **1995**, 67, 1818.
- [8] J. M. Tu, D. A. Keszler, *Mater. Res. Bull.* **1995**, 30, 209.
- [9] S. Lei, Q. Huang, Y. Zheng, A. Jiang, C. Chen, *Acta Crystallogr.* **1989**, 45, 1861.
- [10] S. C. Wang, N. Ye, W. Li, D. Zhao, *J. Am. Chem. Soc.* **2010**, 132, 8779.
- [11] W. L. Zhang, W. D. Cheng, H. Zhang, L. Geng, C. S. Lin, Z. Z. He, *J. Am. Chem. Soc.* **2010**, 132, 1508.
- [12] H. P. Wu, S. L. Pan, K. R. Poepelmeier, H. Y. Li, D. Z. Jia, Z. H. Chen, X. Y. Fan, Y. Yang, J. M. Rondinelli, H. S. Luo, *J. Am. Chem. Soc.* **2011**, 133, 7786.
- [13] M. C. Chen, L. H. Li, Y. B. Chen, L. Chen, *J. Am. Chem. Soc.* **2011**, 133, 4617.
- [14] S. F. Jin, G. M. Cai, W. Y. Wang, M. He, S. C. Wang, X. L. Chen, *Angew. Chem.* **2010**, 122, 5087; *Angew. Chem. Int. Ed.* **2010**, 49, 4967.
- [15] R. K. Li, *J. Non-Cryst. Solids* **1989**, 111, 199.
- [16] C. T. Chen, Z. Y. Xu, D. Q. Deng, J. Zhang, G. K. L. Wong, *Appl. Phys. Lett.* **1996**, 68, 2930.
- [17] C. T. Chen, N. Ye, J. Lin, J. Jiang, W. R. Zeng, B. C. Wu, *Adv. Mater.* **1999**, 11, 1071.
- [18] C. T. Chen, G. L. Wang, X. Y. Wang, Z. Y. Xu, *Appl. Phys. B* **2009**, 97, 9.
- [19] T. Kiss, F. Kanetaka, T. Yokoya, T. Shimojima, K. Kanai, S. Shin, Y. Onuki, T. Togashi, C. Zhang, C. T. Chen, S. Watanabe, *Phys. Rev. Lett.* **2005**, 94, 057001.
- [20] J. D. Koralek, J. F. Douglas, N. C. Plumb, J. D. Griffith, S. T. Cundiff, H. C. Kapteyn, M. M. Murnane, D. S. Dessau, *Phys. Rev. Lett.* **2006**, 96, 017005.
- [21] T. K. Bera, J. H. Song, A. J. Freeman, J. I. Jang, J. B. Ketterson, M. G. Kanatzidis, *Angew. Chem.* **2008**, 120, 7946; *Angew. Chem. Int. Ed.* **2008**, 47, 7828.
- [22] T. K. Bera, J. I. Jang, J. B. Ketterson, M. G. Kanatzidis, *J. Am. Chem. Soc.* **2009**, 131, 75.
- [23] Crystal data for $\text{NaSr}_3\text{Be}_3\text{B}_3\text{O}_9\text{F}_4$: $M_r = 565.31$, colorless block, $0.22 \times 0.14 \times 0.14 \text{ mm}^3$, trigonal, space group $R\bar{3}m$, $a = 10.4466(13)$, $c = 8.3093(17) \text{ Å}$, $V = 785.3(2) \text{ Å}^3$, $Z = 3$, $\rho_{\text{calc}} = 3.586 \text{ g cm}^{-3}$, graphite-monochromatized Mo K_α ($\lambda = 0.71073 \text{ Å}$) on a Rigaku AFC10 diffractometer equipped with a Saturn CCD detector, $F(000) = 780$, $\mu = 15.374 \text{ mm}^{-1}$, $T = 93(2) \text{ K}$, 2821 measured reflections and 639 independent reflections in the range $0.33 < 2\theta < 30.98^\circ$, $R(\text{int}) = 0.0650$; $R1 = 0.0271$ and $wR2 = 0.0632$ for $F_o^2 > 2\sigma(F_o^2)$; $R1 = 0.0305$ and $wR2 = 0.0641$ for all F_o^2 , residual electron density between -0.733 and 0.867 e Å^{-3} , GOF = 0.640. The collection of the intensity data, cell refinement, and data reduction were carried out with the program CrystalClear. Face-indexed absorption correction was performed numerically with the program XPREP. The structure was solved with direct methods implemented in the program SHELXS and refined with the least-squares program SHELXL of the SHELXTL-PC suite of programs. The final refinement included anisotropic displacement parameters. The program STRUCTURE TIDY was then employed to standardize the atomic coordinates. Further details on the crystal structure investigations may be obtained from the Fachinformationszentrum Karlsruhe, 76344 Eggenstein-Leopoldshafen, Germany (fax: (+49) 7247–808–666; e-mail: crysdata@fiz-karlsruhe.de), on quoting the depository number CSD-423143. Rigaku (2008). CrystalClear. Rigaku Corporation, Tokyo, Japan; G. M. Sheldrick, *Acta Crystallogr. Sect. A* **2008**, 64, 112; L. M. Gelato, E. J. Parthé, *Appl. Crystallogr.* **1987**, 20, 139.
- [24] E. Brese, M. O'Keefe, *Acta Crystallogr. Sect. B* **1991**, 47, 192.
- [25] I. D. Brown, D. Altermatt, *Acta Crystallogr. Sect. A* **1985**, 41, 244.
- [26] S. K. Kurtz, T. T. Perry, *J. Appl. Phys.* **1968**, 39, 3798.
- [27] P. Becker, *Adv. Mater.* **1998**, 10, 979.
- [28] M. H. Lee, C. H. Yang, J. H. Jan, *Phys. Rev. B* **2004**, 70, 235110.
- [29] C. T. Chen, Z. S. Lin, Z. Z. Wang, *Appl. Phys. B* **2005**, 80, 1.
- [30] M. C. Payne, M. P. Teter, D. C. Allan, T. A. Arias, J. D. Joannopoulos, *Rev. Mod. Phys.* **1992**, 64, 1045.
- [31] S. J. Clark, M. D. Segall, C. J. Pickard, P. J. Hasnip, M. J. Probert, K. Refson, M. C. Payne, *Z. Kristallogr.* **2005**, 220, 567.
- [32] J. S. Lin, A. Qtseish, M. C. Payne, V. Heine, *Phys. Rev. B* **1993**, 47, 4174.
- [33] L. Kleinman, D. M. Bylander, *Phys. Rev. Lett.* **1982**, 48, 1425.
- [34] H. J. Monkhorst, J. D. Pack, *Phys. Rev. B* **1976**, 13, 5188.